## Section V.C Trap Design, and Scintillation Light Detection

The ultracold neutron production, confinement, and detection region must satisfy a number of stringent requirements. It must contain the isotopically pure superfluid helium, allow neutrons to pass through such that UCN can be produced, permit long UCN and $^3$He storage times, and it must serve as a detector for the neutron-$^3$He capture events.

At first glance, these requirements seem mutually exclusive, but using knowledge obtained from development work with light collection in acrylic cells [1,2] and experiments such as the UCN magnetic trapping experiment, [3] many of these requirements have been well studied and are understood.

### 1) Overview

A schematic of the heart of the experiment in the main cryostat is shown in Fig. V.C.1. The pair of neutron cells that are placed in the gaps between the three electrodes are shown in Fig. V.C.2. The cells consist of two rectangular acrylic tubes, each with dimensions of approximately 7 cm x 10 cm x 50 cm long. The cold neutron beam enters along the long axis of the cell and passes through either deuterated acrylic or deuterated polystyrene windows attached to each end. The beam exits at the rear of the cell and is

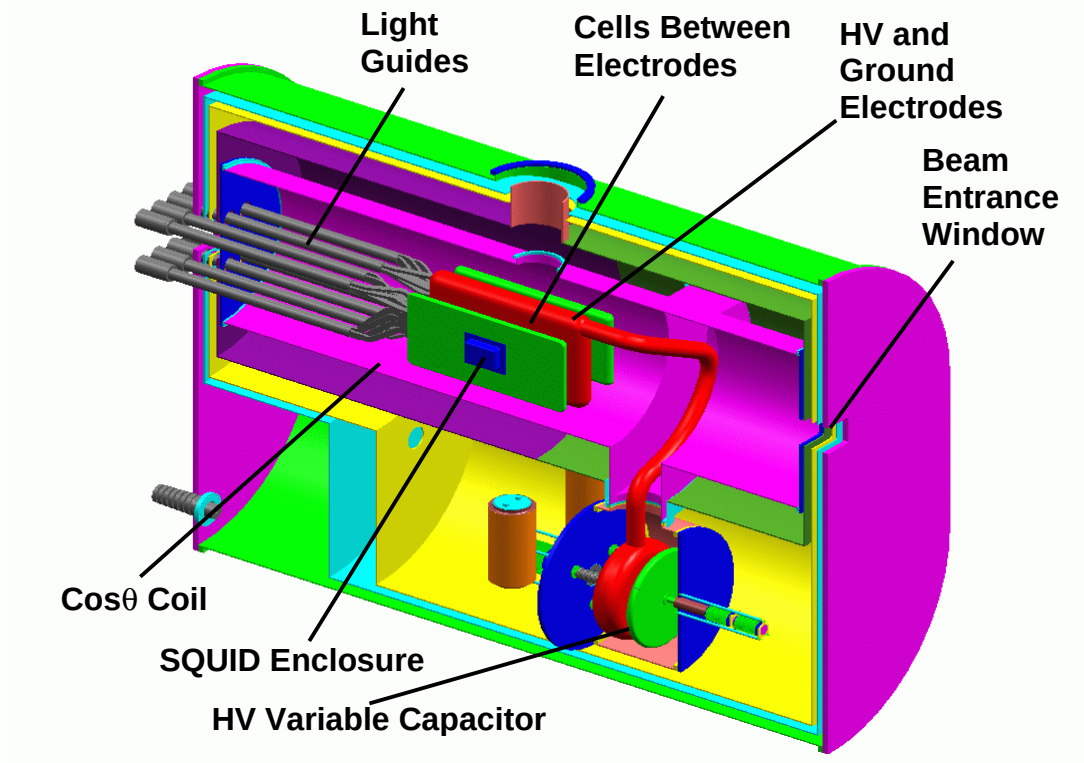


Fig. V.C.1 The UCN production, confinement, and detection region. The neutron beam enters from the right; the internal neutron guides are not shown. The two rectangular cells are placed between the three electrodes. The light guides connect to the PMT's at room temperature.

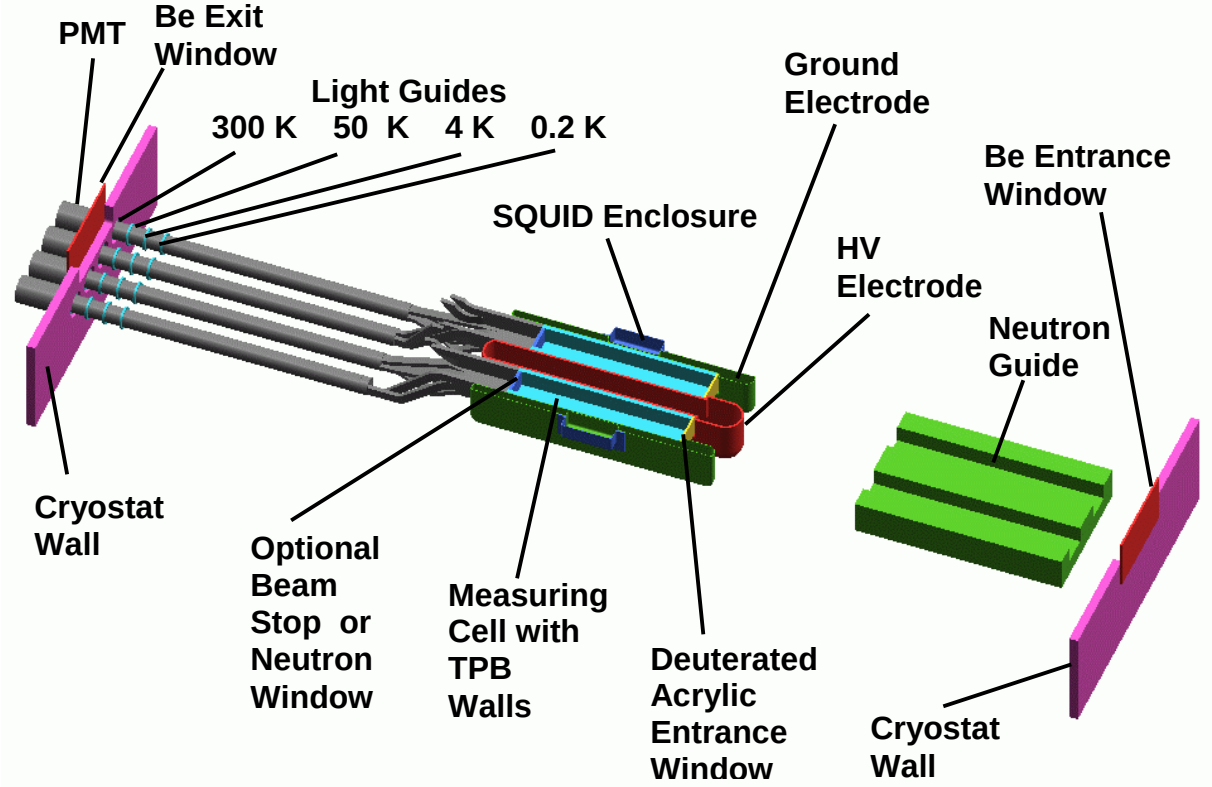


Fig. V.C.2 The path of the neutrons through the cryostat. The beam enters from the right. It is about 3.1 m from Cryostat wall to wall.

absorbed outside the cell in a beam stop made from a neutron absorbing material. The choice of whether to use a transparent or opaque beam stop will be determined based on the detection efficiency of the system.

The collection and measurement sequence has been described in Chapter IV. After the cells are loaded with a mixture of superfluid $^4$He and polarized $^3$He, they are irradiated with polarized cold neutrons to produce polarized UCN that must be confined by the material walls of the cell. After the beam has been switched off, the UCN and $^3$He spin vectors are rotated into the plane perpendicular to the magnetic field and precess until the UCN are either captured by $^3$He or lost due to other processes (beta decay, wall losses, or through small gaps). When the UCN are captured on $^3$He, scintillation light is produced. This light is converted to visible wavelengths and transported out of the detection region and detected using room temperature photomultiplier tubes (PMTs). This process could be repeated until the $^3$He becomes sufficiently depolarized, which could be a single neutron measurement cycle, at which time the cell is emptied and refilled with the $^4$He / $^3$He mixture. This section discusses the UCN confinement, $^3$He depolarization, and transport and detection of scintillation light.

**2) UCN production and confinement**

The UCN are produced inside the acrylic cell through the inelastic scattering (super-thermal) process discussed in Section V.B and [4]. The number of UCN confined is a function of the production rate, the confinement potential of the material surfaces, and the lifetime of UCN in the bottle.

We plan to use walls made from acrylic and coated with deuterated polystyrene doped with a deuterated wavelength shifter (discussed below). The deuterated polystyrene has a UCN potential of 134 neV and should provide a storage lifetime of 500 s due to wall losses and beta decay . The UCN will retain the same polarization sense of the incident neutron and will travel undisturbed in the helium. The UCNs should not depolarize significantly when reflecting from the material walls; typical depolarization rates for plastics are ~ $10^{-6}$ per reflection from the wall[5].

A series of test runs were performed at LANSCE in the spring of 2002 to study the production and to measure the storage time of UCN in an acrylic cell coated with deuterated polystyrene. Although the results are preliminary, they indicate that the production rate obtained is consistent with the theoretically predicted rate within a factor of two. The storage time of UCN in the cell was measured to be 180 (+500, -60) s, consistent with the lifetime of 170 s expected from the calculated UCN leakage through the helium fill hole.

**3) $^3$He depolarization**

A cell that allows for both long UCN storage times and long $^3$He relaxation times (~$10^4$ s, ~ 80 h) is a critical need of the experiment. Past work in this area indicates that sufficiently long relaxation times may be possible, but test experiments will be required to determine the achievable relaxation time for the materials and conditions of the EDM experiment. These tests would be most easily carried out using polarized $^3$He produced by metastability-exchange optical pumping, and may be performed at LANSCE or NIST.

To reduce wall relaxation at cryogenic temperatures, one seeks a suitable diamagnetic material with a low value for E, the energy of adsorption for $^3$He. Although cesium has the lowest value, E = 2.3 K [6], and has been shown to suppress wall relaxation of the $^3$He at the temperatures of interest, cesium is not a suitable coating material because of its large neutron absorption cross section. The next most effective coatings are hydrogen (E=12 K) and deuterium (E=20 K), but only deuterium would be compatible with long UCN storage times. A relaxation time of 128 h was obtained for a 0.07% solution of polarized $^3$He in liquid $^4$He, stored in a hydrogen-coated glass cell at a temperature of 4.2 K and a magnetic field of 3 mG [7]. A relaxation time of about 100 h has also been measured for a gaseous mixture of $^3$He and $^4$He (total density $10^{17}$ cm$^{-3}$) that was stored in a hydrogen-coated, 3-cm diameter glass cell at a temperature of 4 K and magnetic field of 14 G. The relaxation time decreases rapidly at lower temperatures, but recovers to about 1000 s at 0.5 K because of the formation of a

superfluid layer [8, 9]. (Longer relaxation times have been obtained with magnetic fields of 10 kG, but those results are inappropriate for the low magnetic field of the EDM experiment [9].) The hydrogen coating is still required to obtain this relaxation time, but other coatings were not tested. A deuterium coating[10], along with the superfluid layer, might be effective, and would be compatible with the UCN's interaction cross sections. The relaxation time for the large cells discussed here would be enhanced because they would be expected to scale inversely with the surface to volume ratio.

**4) Operating Temperature**

As discussed in Ref. 11, the operating temperature is determined by the requirement that the motion of the $^3$He is free enough so that there will be adequate motional averaging of the magnetic field fluctuations. The $^3$He relaxation time, $T_2$ is a function of the magnetic field gradient, G, the diffusion constant, D, and the length of the cell, L,

$$T_2 = 120\ D / \gamma^2 G^2 L^4$$

and is the limiting parameter in selecting the operating temperature. From Fig. V.C.3 one can see that with a gradient of G = (1-2) x $10^{-7}$ G/cm, a working temperature of 0.4 K is reasonable. However achieving a gradient of G = (1-2) x $10^{-7}$ G/cm is very challenging. On the other hand G = (1-2) x $10^{-6}$ G/cm has been demonstrated many times. The constraints on

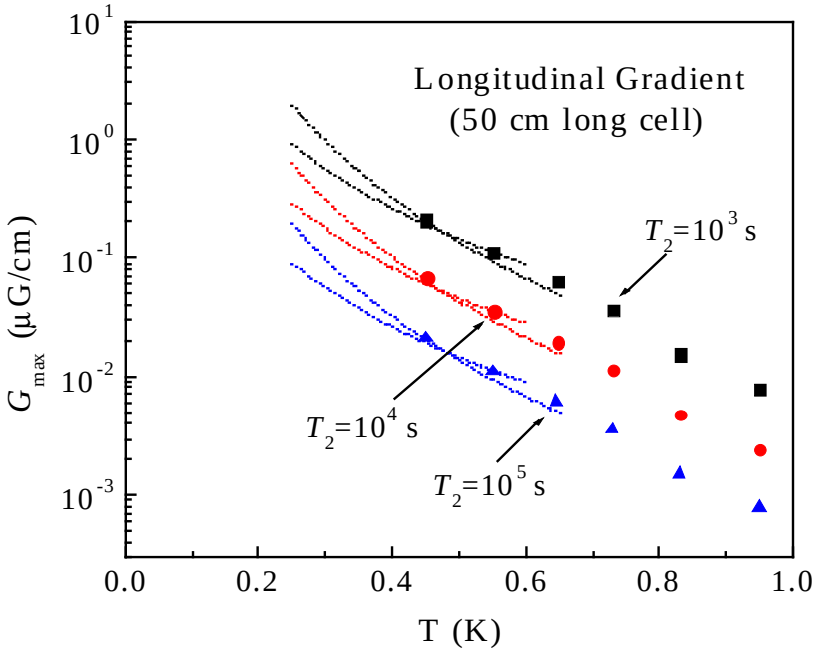


Fig. V.C.3 The maximum permissible gradients in magnetic field as a function of temperature. The gradients are limited by the relaxation rate $1/T_2$

the allowable gradient become more relaxed when the experiment is operated at lower temperature. On the other hand, operating at higher temperatures makes the experiment technically simpler.

The most effective operating temperature is still an open question. But in the range 0.3 to 0.4 K, the motion of the $^3$He atoms crosses over from diffusive to ballistic. In this regard, the $^3$He v x E systematic, described in Section V.H.2, has a rapid change in magnitude, and at some temperature in this range, the $^3$He and UCN systematics are equal. Thus, there is some motivation to operate the experiment at several temperatures to address systematic effects. In addition the temperature dependence of the $^3$He polarization lifetime needs to be studied.

**5) Detection System**

The detection system converts the extreme ultraviolet (EUV) scintillation photons produced by helium scintillations to blue photons, pipes them out of the apparatus, and detects them with room temperature photo-multipliers. Each of these functions will be described below.

EUV light (80 nm) is produced by the recoil of the charged proton and triton from the capture of neutrons by $^3$He when they pass through the superfluid helium. The UCN confinement region is surrounded by 1-cm thick acrylic plates on each of the four sides perpendicular to the beam axis, that aid in transporting this scintillation light out of the apparatus. On the inner surface of the acrylic, the walls are coated with deuterated polystyrene doped with the deuterated organic fluor 1,1,4,4-tetraphenyl buta-1,3-diene (dTPB). The dTPB absorbs the EUV photons and emits blue light with a spectrum peaked at 440 nm and a width of approximately 50 nm [12]. This blue light is transported via total internal reflection through the light guides to the PMTs. The fluorescence efficiency (FE) of TPB doped into a polystyrene matrix is 1.0 relative to Sodium Salicylate [2], which has been independently measured to have an absolute FE of 0.37 [13]. We expect deuterated versions to have a similar FE.

Attached to the detector end of the confinement region are four acrylic light guides that transport the light captured in the ultraviolet transmitting (UVT) acrylic walls to photo-multipliers at room temperature. As the light exits the low-temperature region (< 500 mK) of the apparatus, three short breaks in the light guide will be required to minimize the heat loads on the cell from the warmer surroundings. First, an acrylic window mounted to the 4 K shield provides a separation between the low-temperature region and the 4K shield. The scintillation light will pass through this window while blocking blackbody radiation from the 50 K shield. The second break is between this window and the light guide thermally attached to the 50 K shield. This second light guide transports the light to detectors located at room temperature. The nature of the design - four separate light guides attached to each cell - provides a natural means to allow the use of coincidence detection techniques between two or more PMTs. This will be required because of background events that are discussed further below.

From measurements of neutron capture events in helium [1], the size of a scintillation pulse at any one of the four PMTs is expected to be only a few photoelectrons. These measurements were taken in conditions similar to the conditions of this experiment, but without the magnetic and large electric fields. Tests will need to be performed to determine the detection efficiency in the presence of these fields.

Because of backgrounds, the PMTs must have good gain dispersion. This can be accomplished using a bialkali PMT such as the Burle 8850. These tubes have gain dispersions such that one can have separation between single photoelectron events and multi-photoelectron events. In addition, discrimination between photon scattering events and neutron capture events may be possible.

Tests with a hydrogenated cell at higher temperatures have shown that very good discrimination against gamma rays can be achieved by correlating the number of afterpulses with pulse height. (Afterpulses arise from long-lived excited states in the helium, some decaying with time constants as long as several seconds [14].) It is also important to investigate this discrimination technique at temperatures and magnetic fields appropriate for the experiment.

**6) Backgrounds**

The detector system is developed to have as large as possible light collection efficiency. Since the liquid helium is an efficient scintillator for all forms of ionizing radiation, this also has the down side that a large number of background events are detected from other reactions such as excitations in a variety of locations outside a storage cell itself: inside the helium surrounding the confinement region, inside of the acrylic light guides, or in the PMTs themselves. In general, this light results from a variety of physical processes such as scintillation, luminescence, and Cherenkov radiation.

The primary source of backgrounds is expected to arise from the interaction of neutrons with materials in the apparatus [3]. During the filling phase of the experiment, large ($10^{10}$ - $10^{12}$) numbers of neutrons must be introduced into the apparatus in order to produce UCN. These neutrons will interact with various materials in addition to the $^4$He. If such an interaction results in the storage of energy in a meta-stable state (such as a radioactive isotope or a color center), then the release of that energy can result in background events once the beam is turned off. These events are generally time dependent, so one must carefully test all materials used in the regions exposed to neutrons. Various types of both active and passive background shielding will also be used.

The background events consist primarily of gammas from various sources (such as the radioactive decay of irradiated materials) that Compton scatter to produce betas. These events must be discriminated from the signal produced by the neutron capture on $^3$He. Conventional pulse shape discrimination techniques use either integration or integration and differentiation of the PMT signals with respect to time (e.g. the zero-time crossover method) to make these cuts. This technique however, breaks down when the intensity of the signal becomes low or shows no shape dependence as in the case of neutron-induced scintillations in liquid helium. However the helium scintillations do produce afterpulses that show up as single photon events after the primary signal and have time constants up to several seconds. One possible method to differentiate the helium events from Compton scattering events is to use the initial main pulse as the signal event and require a certain number of afterpulses to follow. For low afterpulse counting rates in the presence of electronic noise, this method is more sensitive than just integrating the signal over the afterpulse time interval.

In a series of experiments [1]; scintillations in liquid $^4$He were produced by a neutron beam with and without a small admixture of $^3$He. Figure V.C.4 shows the probability distribution for scintillation events where the vertical axis corresponds to the pulse height of the main pulse and the horizontal axis gives the number of afterpulses. The upper plot corresponds to the case when the storage cell is filled with pure $^4$He and the lower plot is that of the $^3$He - $^4$He mixture. Afterpulses were counted for 4.5 μs after the primary pulse. Gamma rays that have the same pulse height as neutrons can clearly be discriminated against by placing a condition on the number of afterpulses for each event. Gamma discrimination based on afterpulse counting has only been tested in the high temperature region (2 K) with a hydrogenated cell, so it will be important to investigate this discrimination technique at lower temperatures and higher magnetic fields appropriate for the experiment.

Since gamma radiation from neutron activation by cold neutrons is expected to be a main source of background, neutron shielding will be used to minimize irradiation of different materials by the scattered cold beam. Unfortunately, the functions of certain parts of the apparatus, such as windows for introducing neutrons into the apparatus, and the down converting fluor and acrylic portions of the detection system, necessitates that they be unshielded from neutrons. These materials must then be selected with extreme care to minimize neutron activation of impurity elements. The materials in the electrodes are especially critical in this regard due to their proximity to the neutron cells. Copper films evaporated on a suitable substrate are being considered as electrode construction materials (Section V.G).

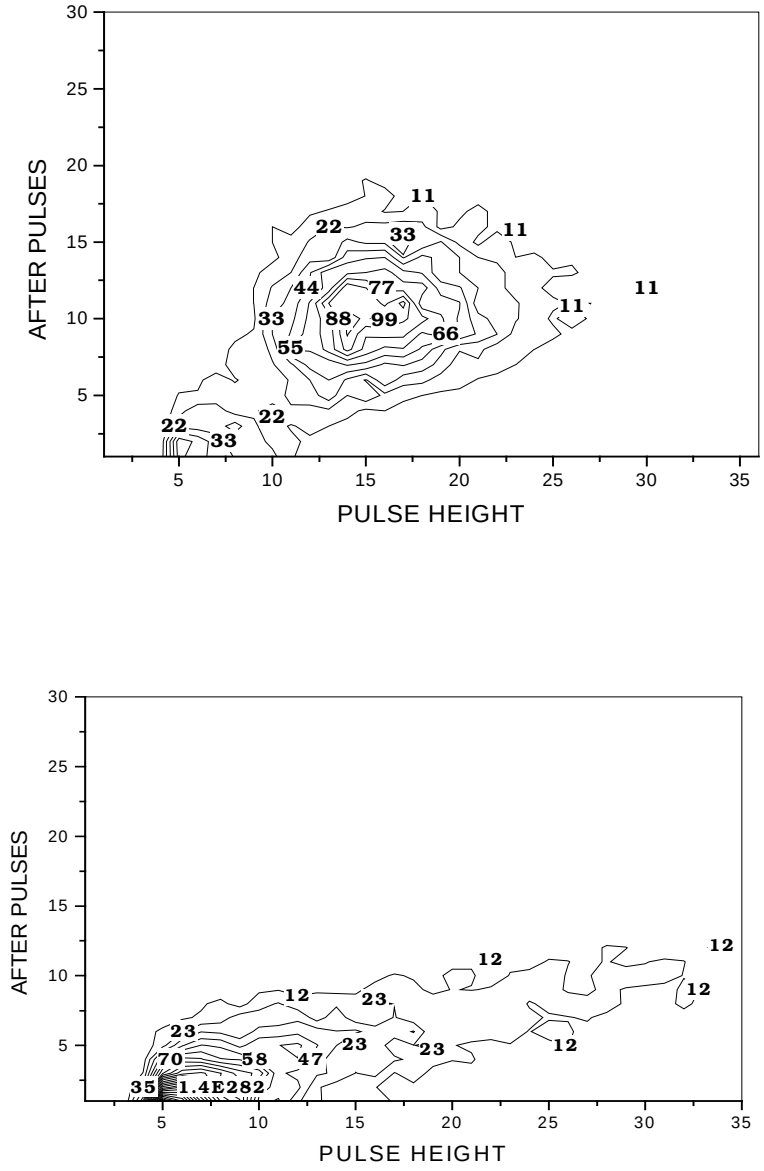


Fig. V.C.4 Tests at 1.8K have shown that very good discrimination against gamma rays can be achieved by correlating the number of afterpulses with the main pulse height. Both plots show data taken with a cold neutron beam. The upper plot shows the probability distribution of scintillation events when the cell was filled only with pure $^4$He; the lower plot shows data for a mixture of $^3$He / $^4$He.

Luminescence of materials can be easily removed through the use of coincidence detection because these events are uncorrelated single photon emissions. Nevertheless, materials used for neutron shielding may need opaque materials placed between them and the photo-multipliers to minimize the detection of luminescence light through spurious coincidence.

External shielding will be used to minimize ambient backgrounds to which the experiment is susceptible, such as external gamma and cosmic radiations. Active vetoing of cosmic ray muons will be performed using scintillation paddles.

**References**


[1] K. Habicht, *Szintillationen in flüsrigen Helium – ein Detektor für ultrakalte Neutronen*, Ph.D. Thesis, Technischen Universitåt Berlin, 1998.
[2] D. N. McKinsey *et al*., *NIM* **B 132**, 351 (1997).
[3] P.R. Huffman *et al.*, *Nature* **403**, 62 (2000).
[4] R. Golub and J. M. Pendlebury, *Phys. Lett*. **62A**, 337 (1977).
[5] A. Serebrov *et al*., *NIM* **A440**, 717 (2000).
[6] G. Tastevin, *J. Low Temp. Phys*. **89**, 669 (1992).
[7] M. A. Taber, *J. Physique*, **39**, C6-192 (1978).
[8] M. Himbert and J. Dupont-Roc, *J. Low Temp. Phys*. **76**, 435 (1989).
[9] C. Lusher, M. Secca, and M. Richards, *J. Low Temp. Phys*. **72**, 71 (1988).
[10] V. Lefevre-Sequin *et al., J. Physique* **46**, 1145 (1985).
[11] R. Golub and S. K. Lamoreaux, *Phys. Rep*. **237**, 1 (1994).
[12] W. M. Burton and B.A. Powell, *Appl. Opt*. **12**, 87 (1973).
[13] E. C. Bruner Jr., *J. Opt. Soc. Am*. **59**, 204 (1969).
[14] D. N. McKinsey *et al*., *Phys. Rev.* **A59**, 200 (1999).